

## Identification of Phosphinate Dipeptide Analog Inhibitors Directed against the *Plasmodium falciparum* M17 Leucine Aminopeptidase as Lead Antimalarial Compounds

Tina S. Skinner-Adams,<sup>†,‡</sup> Jonathan Lowther,<sup>§</sup> Franka Teuscher,<sup>†</sup> Colin M. Stack,<sup>§</sup> Jolanta Grembecka,<sup>||</sup> Artur Mucha,<sup>⊥</sup> Pawel Kafarski,<sup>⊥</sup> Katharine R. Trenholme,<sup>†</sup> John P. Dalton,<sup>§</sup> and Donald L. Gardiner<sup>\*,†</sup>

Malaria Biology Laboratory, Queensland Institute of Medical Research, 300 Herston Road, Herston, Queensland, 4029, Australia, Department of Medicine, Central Medical Division, University of Queensland, Brisbane, 4072, Australia, Institute for the Biotechnology of Infectious Diseases, University of Technology Sydney, Corner of Thomas and Harris Street, Ultimo, Sydney, NSW 2007, Australia, Department of Molecular Physiology and Biological Physics, University of Virginia, Charlottesville, Virginia 22904, and Department of Bioorganic Chemistry, Faculty of Chemistry, Wrocław University of Technology, Wyspińskiego 27, 50-370 Wrocław, Poland

Received June 22, 2007

Previous studies have pinpointed the M17 leucyl aminopeptidase of *Plasmodium falciparum* (PfLAP) as a target for the development of new antimalarials. This metallo-exopeptidase functions in the terminal stages of hemoglobin digestion and is inhibited by bestatin, a natural analog of Phe-Leu. By screening novel phosphinate dipeptide analogues for inhibitory activity against recombinant PfLAP, we have discovered two compounds, **4** (hPheP[CH<sub>2</sub>]Phe) and **5** (hPheP[CH<sub>2</sub>]Tyr), with inhibitory constants better than bestatin. These compounds are fast, tight-binding inhibitors that make improved contacts within the active site of PfLAP. Both compounds inhibit the growth of *P. falciparum* in vitro, exhibiting IC<sub>50</sub> values against the chloroquine-resistant clone Dd2 of 20–40 and 12–23 μM, respectively. While bestatin exhibited some in vivo activity against *Plasmodium chabaudi chabaudi*, compound **4** reduced parasite burden by 92%. These studies establish the PfLAP as a prime target for the development of antimalarial drugs and provide important new lead compounds.

### Introduction

Malaria is the disease caused by apicomplexan parasites of the genus *Plasmodia*, with *Plasmodium falciparum* being the most lethal of the four *Plasmodium* species infecting man. The annual death toll of this disease has been estimated to be 2–3 million.<sup>1</sup> In 1998 the World Health Organization, UNICEF, UNDP, and the World Bank launched The Roll Back Malaria (RBM) Initiative to provide a coordinated international approach to fighting malaria, with the target of halving the burden of this disease by 2010. However, the dramatic decline in the effectiveness of many antimalarial agents and the increase of insecticide resistance in the vector population is significantly impeding progress. Unfortunately, recent reports indicate that malaria morbidity and mortality have increased since the inception of the program, and it now seems unlikely that it will reach its goal.<sup>2</sup> Accordingly, there is a pressing need to discover and develop new antimalaria drug treatments.

We have proposed the malaria M17 leucyl aminopeptidase (PfLAP<sup>a</sup>), a cytosolic metallo-exopeptidase catalyzing the removal of amino acids from the *N*-terminus of peptides generated during hemoglobin degradation, as a potential target for new antimalarials.<sup>3</sup> Amino acids derived from hemoglobin are essential to parasite protein synthesis, and hence to their growth and development within the host erythrocyte.<sup>4</sup> Recently, we showed that recombinant PfLAP is inhibited by the antibiotic bestatin, a natural analog of the dipeptide Phe-Leu derived from

*Streptomyces olivoreticuli*.<sup>5</sup> Bestatin also inhibited the in vitro growth of *P. falciparum*, but was less effective against transgenic parasites that overexpressed PfLAP.<sup>3</sup>

Highly potent organophosphorus inhibitors of aminopeptidases have been designed and synthesized in our laboratory.<sup>6</sup> In the present study, these compounds were screened against a functionally active recombinant PfLAP. We identified two phosphinate dipeptide analogues, **4** (hPheP[CH<sub>2</sub>]Phe) and **5** (hPheP[CH<sub>2</sub>]Tyr), with superior binding kinetics to rPfLAP than bestatin and with killing activity against malaria parasites in culture. More importantly, while bestatin exhibited some antimalarial activity in vivo against the rodent malaria *Plasmodium chabaudi chabaudi*, compound **4** reduced parasite burden in infected mice by 92%. These studies establish PfLAP as a new antimalarial drug target and identify valuable dipeptide analogues that can be used as lead compounds for future drug design and development.

### Results

**rPfLAP Is Inhibited by Bestatin and Phosphinate Analogues of Dipeptides.** A panel of phosphinate analogues of dipeptides<sup>6</sup> were screened for inhibitory activity against a functionally active recombinant PfLAP.<sup>5</sup> Four of these analogues were selected for further study (compounds **2–5**, Table 1) because they exhibited strong inhibition of rPfLAP ( $K_i < 1 \mu\text{M}$ ); compounds **4** and **5** were the most potent, with  $K_i$  values better than that of bestatin (Table 1).

The mode by which compounds **4** and **5** inhibit rPfLAP differs from that of bestatin; this difference was revealed by the shape of the reaction curves between enzyme (E) and inhibitor (I) (Figure 1A,B; only compound **4** is shown). Arrival at steady-state reaction rates was time-dependent for bestatin, demonstrating that this compound is a slow-binding inhibitor of rPfLAP. The dissociation constant ( $K_i$ ) for the formation of the initial EI complex was calculated to be 425 nM, while the

\* Corresponding author. Phone: +61-7-33620432. Fax: +61-7-33620104. E-mail: donG@qimr.edu.au.

<sup>†</sup> Queensland Institute of Medical Research.

<sup>‡</sup> University of Queensland.

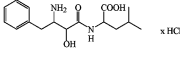
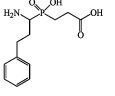
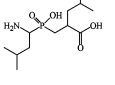
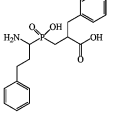
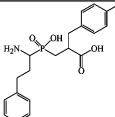
<sup>§</sup> University of Technology Sydney.

<sup>||</sup> University of Virginia.

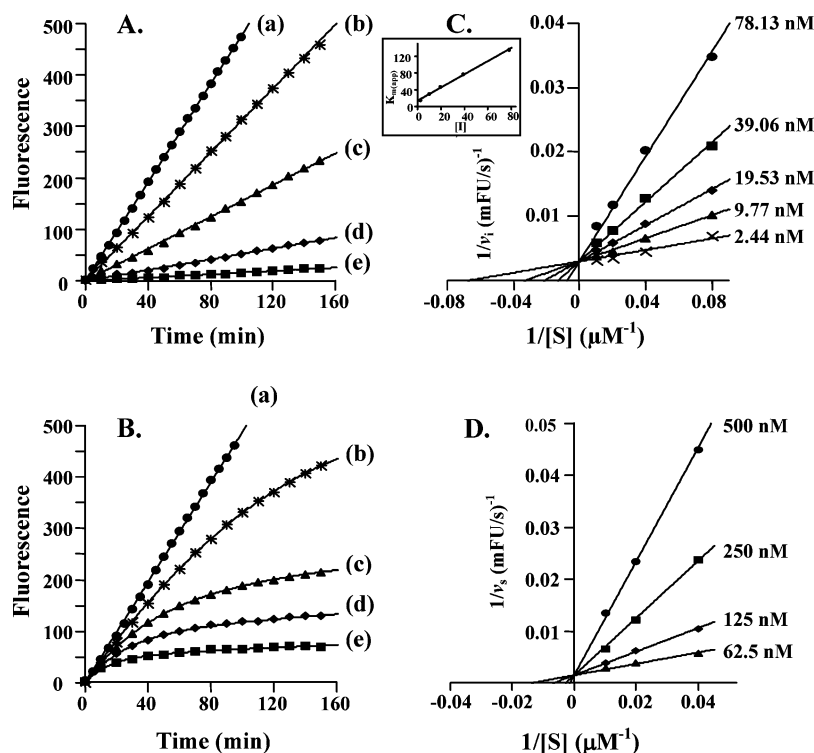
<sup>⊥</sup> Wrocław University of Technology.

<sup>a</sup> Abbreviations: PfLAP, leucyl aminopeptidase of *Plasmodium falciparum*; B1LAP, bovine lens aminopeptidase.

**Table 1.** Data Describing the Inhibition Characteristics of Bestatin and the Phosphinic Acid Dipeptide Analogues When Assessed against *rPfLAP* and *pkLAP* and *P. falciparum* Parasites in Continuous Culture

Inhibitor	Antimalarial activity <i>in vitro</i>	IC <sub>50</sub> (μM)			<i>rPfLAP</i>	<i>pkLAP</i>
		Dd2	D10	3D7	K <sub>i</sub> ± SE (nM)	K <sub>i</sub> (nM)
Bestatin (Phe[CHO]Leu, 1)		12-21	11-15	8-14	25±1.2 <sup>a</sup>	20 <sup>b</sup>
hPheP[CH <sub>2</sub> ]Gly (2)		>100	>100	>100	524.8±10.3	ND
LeuP[CH <sub>2</sub> ]Leu (3)		>100	>100	>100	97.3±5.2	110 <sup>c</sup>
hPheP[CH <sub>2</sub> ]Phe (4)		20-40	46-75	24-62	13.2±0.5	66 <sup>c</sup>
hPheP[CH <sub>2</sub> ]Tyr (5)		13-23	47-62	19-28	10.4±0.9	67 <sup>c</sup>

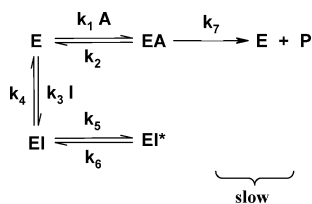
<sup>a</sup> K<sub>i</sub><sup>\*</sup>: overall inhibition constant for bestatin calculated from steady-state rates; see results in the text. <sup>b</sup> Nishizawa et al. 1977. <sup>c</sup> Reference 6. ND, not determined.



**Figure 1.** Comparison of kinetics of inhibition of *PfLAP* by compound **4** and bestatin. (A and B) Progress curves for the hydrolysis of H-Leu-NHMeC by *rPfLAP* in the presence of increasing concentrations of compound **4** (A) and **1** (B). The final concentrations of substrate and enzyme were 2 μM and 26 nM, respectively. The final concentrations of compound **4** were (a) 0 nM, (b) 4.88 nM, (c) 19.53 nM, (d) 78.13 nM, and (e) 312.5 nM. The final concentrations of **1** were (a) 0 nM, (b) 19.53 nM, (c) 78.13 nM, (d) 156.25 nM, and (e) 312.5 nM. Double-reciprocal plots for inhibition of *rPfLAP* by compound **4** (C) (final concentration of enzyme was 26 nM, while the substrate concentrations were 12.5, 25, 50, and 100 μM) and bestatin (D) (final concentration of enzyme was 22 nM, while the substrate was at 25, 50, and 100 μM). (Inset) Plot of apparent *K<sub>m</sub>* against compound **4** inhibitor concentration [I].

overall inhibition constant (*K<sub>i</sub><sup>\*</sup>*) for formation of EI\* was calculated to be 25 nM (Table 1). The observed rate constants *k<sub>obs</sub>* for the formation of EI\* were calculated by fitting the

progress curve data and, when plotted against [I], gave a positive hyperbolic plot, indicating that bestatin binds to *rPfLAP* according to the mechanism shown in Scheme 1.<sup>7</sup> Therefore,

**Scheme 1.** Mechanism for Slow-Binding Inhibition of *rPflAP* by Bestatin

while formation of the initial EI complex between *rPflAP* and bestatin is fast, the formation of the final EI\* complex is slow and may require conformational change in the substrate and/or active site of the enzyme.

In contrast to bestatin, rates of substrate hydrolysis by *rPflAP* in the presence of increasing concentrations of **4** or **5** were linear, indicating that equilibrium between the enzyme and these inhibitors is reached rapidly (compare parts A and B of Figure 1; only compound **4** is shown) and that these compounds are tight-binding inhibitors of *rPflAP* (Figure 1A). Lineweaver–Burk plots demonstrate that **4** and **5** act through competitive inhibition (Figure 1C). By plotting  $K_{m(\text{app})}$  values calculated from the  $x$ -axis intercepts of the Lineweaver–Burk plot at different inhibitor concentrations against  $[\text{I}]$ , a Michaelis–Menten constant,  $K_m$ , of 13  $\mu\text{M}$  was obtained for the enzyme (inset in Figure 2C). The  $K_i$  for the inhibition of *rPflAP* by **4** and **5** was calculated to be 13.2 and 10.4 nM, respectively (Table 1), demonstrating that these compounds have a >2-fold better inhibitory activity against *rPflAP* than bestatin ( $K_i$  value of 25 nM). Importantly, these two compounds showed a 5–6-fold better inhibitory activity against *rPflAP* compared to porcine kidney M17 leucyl aminopeptidase (pkLAP) (Table 1).

Compounds **2** (hPheP[CH<sub>2</sub>]Gly) and **3** (LeuP[CH<sub>2</sub>]Leu) exhibited far less inhibitory activity ( $K_i = 524.8$  and 97.3 nM, respectively) compared to **4** and **5**, but they proved useful for understanding the structure–activity relationship of the anti-*PflAP* activity of the phosphinate analogues of dipeptides (see below).

**Structure–Activity Relationships Using Homology Model of *PflAP* and Docking with Phosphinate Analogues of Dipeptides.** Like other M17 leucine aminopeptidases, *PflAP* consists of a less conserved N-terminal domain and a more conserved C-terminal domain containing the active site (Figure 2A). The catalytic domain of *PflAP* (residues 280–606) exhibits 38% overall sequence identity and 56% sequence similarity to the catalytic domain of BILAP; therefore, the X-ray structure of this enzyme was used as a template to build the 3D model of *PflAP*. The amino acids involved in the coordination of two catalytic zinc metal ions and other active site residues are conserved between the two enzymes (Figure 2A). The S1 pockets are similar in size and character, but differences were observed in the residues that lie at the bottom of the pocket (F398, L492, and S580 in *PflAP* correspond to A272, D365, and M454 in BILAP). The S1' pockets are identical (Figure 2A).

The binding modes of bestatin and (*R*)-hPheP[CH<sub>2</sub>]-(*R*)-Phe (**4**) to *PflAP* were calculated using the X-ray structures of BILAP in complex with amastatin (1bll in PDB) and *L*-leucinephosphonic acid (LeuP, 1lcp in PDB) as templates, and these binding modes will be subjected to further discussion in this paper. In addition, we carried out “de novo” docking of these inhibitors to *PflAP* to consider potential alternative binding modes of **4** and bestatin to *PflAP* (results described in the Supporting Information). The modeled binding mode of

bestatin to *PflAP* shows that the hydroxyl group of bestatin is coordinated to the two metal ions (Figure 2B). The  $\alpha$ -amino group coordinates to one of these metal ions and also forms a hydrogen bond with D379. The carbonyl oxygen of bestatin is involved in a hydrogen bond with the backbone amide of G489, while the carboxylate oxygen forms a hydrogen bond with the side chain of T488. The hydrophobic side chains at the P1 and P1' positions of bestatin fit well into the corresponding S1 and S1' binding pockets (Figure 2B). Similar interaction patterns of bestatin and amastatin to BILAP were reported in the literature.<sup>8,9</sup>

Docking of compound **4** into the binding site revealed that two oxygen atoms and an amino group are able to interact with both metal ions in the active site of *PflAP* (Figure 2C). In addition, one oxygen atom of **4** forms a hydrogen bond with the side chain of K386, and the N-terminal amino group is involved in a hydrogen bond with the carboxyl group of D379. The C-terminal carboxyl of **4** forms a hydrogen bond with the backbone amide of G489 and with the side chain of T488, while its second oxygen is solvent exposed. The hPhe side chain at the P1 position of **4** fits well into the large hydrophobic S1 pocket of *PflAP*, and the Phe side chain at P1' is well-accommodated at the S1' pocket (Figure 2C). A similar interaction pattern was observed for LeuP with BILAP active site and the S1 pocket.<sup>10</sup>

The low binding affinity of **2** for *PflAP* can be explained by the presence of a small amino acid, Gly, in the P1' position that does not penetrate the S1' pocket sufficiently deeply to make any significant interactions (Figure 2C). The S1 pocket in *PflAP* can easily accommodate the hydrophobic side chains of Leu and hPhe at the P1 position of **3** and **4**, respectively; however, the larger hPhe chain of **4** enables it to make additional contacts with the hydrophobic amino acids at the bottom of the S1 pocket, namely with F398, L492, S580, and L395. In addition, the Phe at position P1' of **4** can be engaged in more hydrophobic contacts with the S1' pocket than **3**, which contains Leu at the corresponding position (Figure 2B,C). Collectively, these increased interactions would account for the greater affinity of **4** for *PflAP* versus **3**. The binding affinity of compound **5** for *PflAP* is comparable to that of compound **4** (Table 1), while the P1 Tyr of **5** possesses an additional hydroxyl that is solvent exposed and not engaged in hydrogen bonding; therefore, no significant enhancement of the binding affinity over compound **4** was expected nor observed.

**The in Vitro Activity of Phosphinate Analogues against *P. falciparum*.** The antimalarial activity of the phosphinate analogues **2–5** were investigated in vitro. Compounds **2** and **3** did not reduce parasite growth in culture, even at concentrations of 100  $\mu\text{M}$ . In contrast, **4** and **5** were active against both drug resistant (Dd2) and drug sensitive (3D7) *P. falciparum* parasites. Both of these compounds displayed similar antimalarial activities, with IC<sub>50</sub> values against the drug resistant clone Dd2 of 20–40 and 12–23  $\mu\text{M}$  for compounds **4** and **5**, respectively (Table 1). These inhibition values were similar to those achieved with bestatin (IC<sub>50</sub> = 12–21  $\mu\text{M}$ ). Although IC<sub>50</sub> values were similar and not statistically different, irrespective of the isolate used, the multidrug resistant clone Dd2 was consistently more sensitive to each of the compounds tested (Table 1).

**In Vivo Antimalarial Activity of **4** and Bestatin.** The clinical significance of the antimalarial activity demonstrated by bestatin and **4** was examined in vivo using a nonlethal murine malaria model. Parasites appeared in the blood of mice treated with PBS on day 5 postinfection and rose to a median peak parasitemia of 44.8% on day 8 before declining (Figure 3). Both

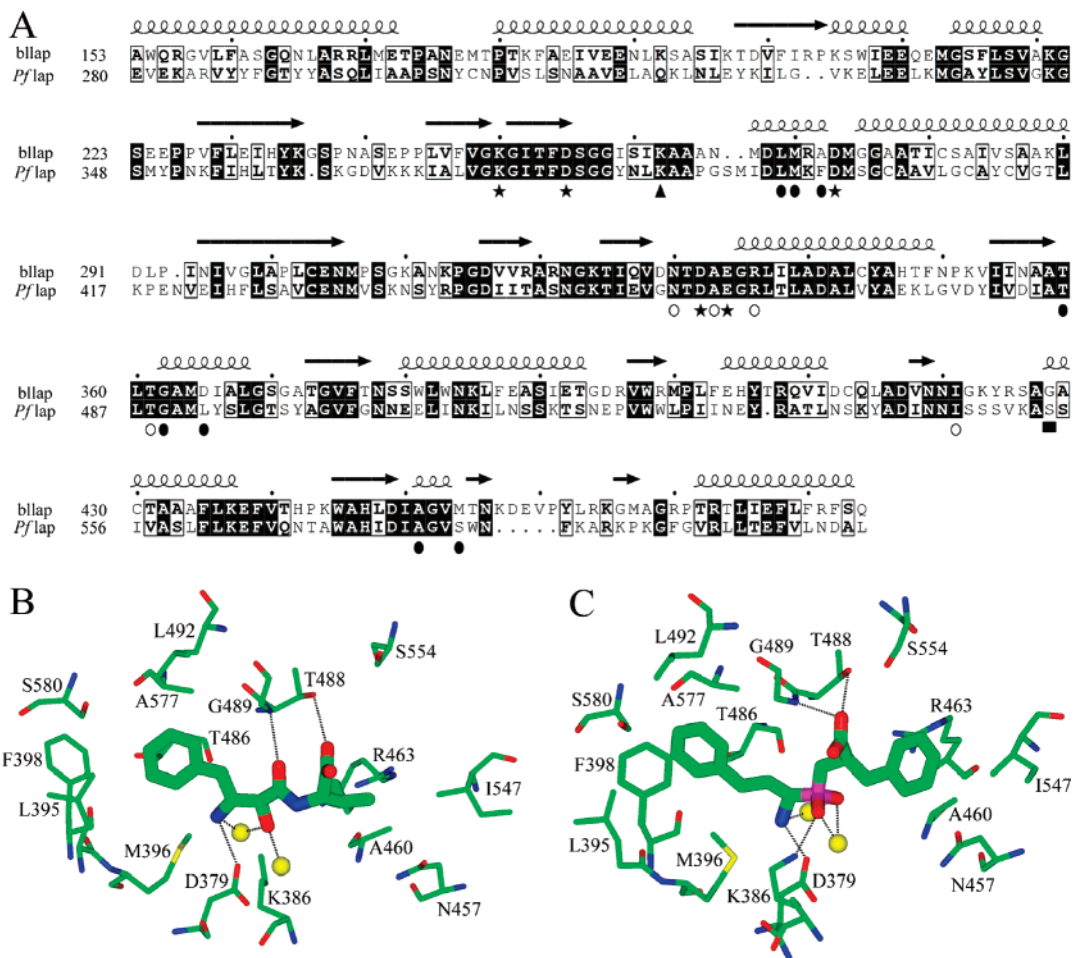


**Figure 2.** (A) Sequence alignment of the catalytic domain of leucine aminopeptidase from *P. falciparum* (*PfLAP*, Pf14\_0439, plamodb.org) with bovine lens leucine aminopeptidase (BILAP, sequence subtracted from PDB file 1lcp) obtained with the ClustalW program. The figure was prepared using the ESPript program (<http://prodes.toulouse.inra.fr/ESPrpt/>). Secondary structures of BILAP: helices (shown as springs) and  $\beta$ -sheets (presented as arrows) are plotted on the top of the alignment. Amino acids conserved in both enzymes are colored white and shown in black boxes, while similar amino acid (similarity defined by default parameters in ESPript) are colored black and shown in white boxes. Amino acids interacting with two metal ions present in the active site of both enzymes are indicated by black stars; black circles show the residues involved in the formation of the S1 pocket; white circles indicate amino acids of the S1' pocket; the black triangle points to K386 in the active site of *PfLAP* engaged in the hydrogen bond with ligands; the black square indicates S554, which is in a hydrogen bond distance to ligands. (B) Modeled interaction mode of compound **4** with *PfLAP*. The S1 and S1' binding pockets and active site residues (thin sticks) involved in interactions with dipeptide analogues (thicker sticks) are shown. Two active site zinc metal ions are represented by yellow spheres. Hydrogen bonds and interactions of the inhibitor with metal ions are shown as black dashed lines. Atoms are colored according to atom types: C, green; N, blue; O, red; S, yellow. (C) Modeled binding mode of bestatin to *PfLAP*. The coloring and labeling is the same as panel B.

bestatin and **4** were effective in reducing the parasitemia of mice infected with *P. chabaudi*. Mice treated with bestatin displayed a reduced median parasitemia of 29.7%, which occurred on the same day as the PBS vehicle control peak parasitemia. Mice treated with **4** exhibited a 3-day delay in the appearance of parasites, and a median peak parasitemia of only 3.6% (representing a 92% reduction compared to PBS controls), which cleared over the subsequent 4 days (Figure 3). Chloroquine treatment delayed the appearance of parasites by 6 days, with a median peak parasitemia of 6.9% on day 14, which cleared over the next 4 days. Similar results were obtained in two separate trials. No toxicity was observed in any of the treatment groups.

## Discussion

To support their rapid growth and development within the erythrocyte, malaria parasites must acquire nutrients from the host cell and the extracellular environment. Although amino acids can be drawn from the host serum, red cell hemoglobin is an essential source of amino acids for parasite protein

anabolism.<sup>11</sup> Cysteine (falcipains) and aspartic (plasmepsins) endopeptidases function within the acidic digestive vacuole (DV) and produce peptides that are transported to the cytosol for further processing by aminopeptidases.<sup>12</sup> We have shown that one of these aminopeptidases, *PfLAP*, functions within the neutral pH environment of the parasite cytosol, can free amino acids from hemoglobin-derived peptides, and is highly expressed in trophozoites, the intraerythrocytic stage at which protein synthesis is at its peak.<sup>5</sup> Inhibitors of *PfLAP*, such as bestatin, exhibit antimalarial activity in vitro, with particular activity against trophozoite stages.<sup>12</sup> Transgenic parasites that overexpress *PfLAP* are also less susceptible to bestatin, supporting our premise that this enzyme is a worthy candidate for investigation as a target for antimalarial development.<sup>3</sup>

Using bestatin as a benchmark, we assessed the inhibitory activity of phosphinate analog against *rPfLAP* and identified two, **4** and **5**, that exhibited a 2-fold greater affinity for the enzyme than bestatin. Since the P1 and P1' side chains of **4** and **5** are larger than the corresponding side chains of bestatin, these can interact with the hydrophobic residues at the bottom

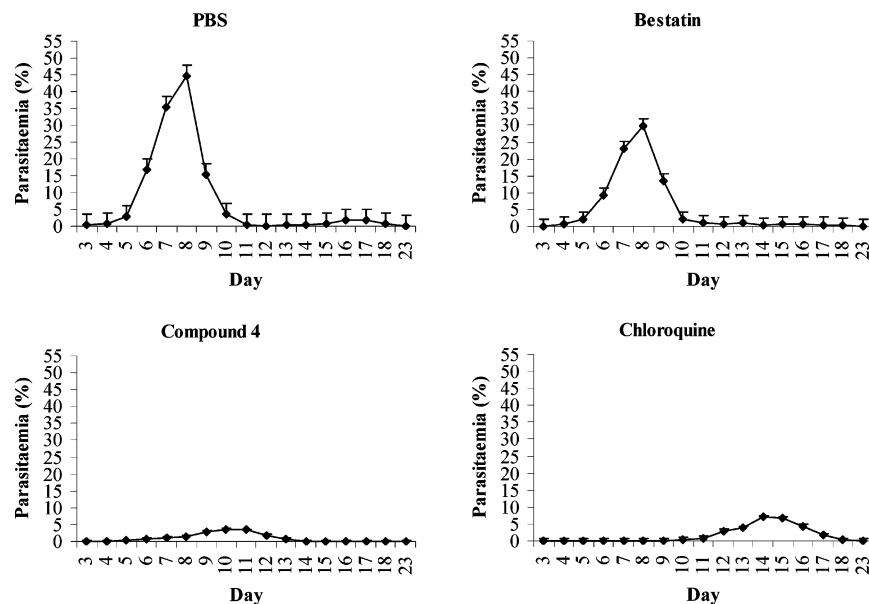


**Figure 3.** In vivo efficacy of compounds **4**, **1**, and chloroquine against *P. c. chabaudi* murine malaria. Data are presented as mean  $\pm$  SE parasitemia for each group of six mice.

of the S1 pocket and with the S1' pocket of the *Pf*LAP. Additionally, unique contacts take place among the phosphinic group, the active site metal ions, and residue Lys386 that do not occur with the corresponding fragment in bestatin. Both of these features account for the high binding affinity of **4** and **5** over bestatin for *Pf*LAP.

Molecular modeling of the phosphinate dipeptide analogues within the active site of *Pf*LAP demonstrated that the size of hydrophobic substituents, both at P1 and P1', influence their binding affinities (Table 1). Simple phosphonic analogues of amino acids (LeuP, hPheP;  $K_i > 10 \mu\text{M}$ ; data not shown) and compound **2** ( $K_i = 524.8 \text{ nM}$ ) were poor inhibitors of *rPf*LAP, suggesting that a larger substitute than Gly at the P1' position is required for inhibition. Indeed, replacement of Gly with a larger and aromatic Phe side chain at P1' in compound **4** resulted in a 40-fold increase in inhibitory potency (Table 1). Simultaneous replacement of Leu at the P1' position by Phe and Leu at the P1 position by hPhe was also significant, as compound **4** had a 7-fold greater binding affinity compared to compound **3** (Table 1). Compound **5** differed from **4** by having a Tyr in the P1' position rather than a Phe, but this did not alter the binding kinetics, since the extra hydroxyl group did not make additional contacts within the active site of *Pf*LAP.

Notwithstanding the similarities in the active site architecture of *Pf*LAP and mammalian LAPs, specificity of binding was observed. For example, the phosphonic analogues of amino acids (LeuP, hPheP) that exhibited poor inhibition of *Pf*LAP are relatively potent inhibitors of porcine kidney leucine aminopeptidase ( $K_i$  values of 230 and 215 nM, respectively).<sup>5,6</sup> More relevantly, compounds **4** and **5** were 5–6-fold more effective against *Pf*LAP as compared to *pkLAP*.<sup>5</sup> The higher affinities of **4** and **5** for *rPf*LAP can be explained by differences in amino acids at the bottom of their S1 pockets, most particularly the presence of F398 and L492 in *Pf*LAP compared to A272 and D365 in *BILAP*. These data argue well for the development of inhibitors that are selective for *Pf*LAP compared to the host enzymes and, hence, have reduced probability of inducing side effects in the host.

The activity of the phosphinate analogues against malaria growth in culture correlated with their inhibitory activity against *rPf*LAP. Compounds **2** and **3** were not effective inhibitors of

parasite growth in vitro, whereas **4** and **5** demonstrated antimalarial activity. However, although the activities of **4** and **5** against *rPf*LAP were 2-fold better than bestatin, their  $\text{IC}_{50}$  values against malaria parasites in culture were similar. This small discrepancy could be explained by differences in their chemical properties, including stability and solubility in aqueous media, and/or differences in their relative ability to penetrate membranes to reach their site of action. Previously described transgenic parasites that overexpress *Pf*LAP<sup>3</sup> are also less susceptible to inhibition by compound **4** or **5** ( $\text{IC}_{50}$  values  $> 100 \mu\text{M}$  and  $88 + 10 \mu\text{M}$ , respectively) compared to wild-type D10 parent parasites ( $\text{IC}_{50}$  values of  $67 + 17$  and  $53.3 + 18 \mu\text{M}$ , respectively) or parasites transfected with a control vector (pHH1 without the AP14cmv cassette) (data not shown), confirming that *Pf*LAP is a target for these phosphinate inhibitors.

We assessed the antimalarial activity of compound **4** in vivo using the rodent *P. c. chabaudi* model. At a treatment dose of 100 mg/kg twice a day, compound **4** reduced parasite burdens in treated mice by 92% compared to controls and, under the regime employed, proved better than treatment with chloroquine (85% reduction in parasitemia). Bestatin treatment (100 mg/kg twice daily) also provided protection, although the parasitemia was reduced by only 34%. The 2-fold increase in the ability of compound **4** to inhibit *rPf*LAP over bestatin would not account for its far superior in vivo antimalarial activity (particularly taking into account their similar in vitro activity). Pharmacokinetic factors including rates of elimination, cellular uptake, and metabolism are likely to be more important. Bestatin enters red blood cells very slowly (0.3%/min in vitro) and is rapidly eliminated from serum (half-life  $> 2 \text{ h}$  in mice).<sup>13</sup> The half-life and tissue and cellular penetration of **4** is not known, but because of its hydrophobicity, these are expected to be significantly greater than those of bestatin. It is also important to note that all of the compounds tested in this study were mixtures of four diastereomers, and it is known that bestatin isomer (2*S*,3*R*)-AHPA-(*R*)-Leu is at least 10-fold more active against *BILAP* than the remaining stereoisomers.<sup>14</sup> Therefore, the activity of the stereoisomers (*R*)-hPheP[CH<sub>2</sub>]-(*R*)-Phe (**4**) and (*R*)-hPheP[CH<sub>2</sub>]-(*R*)-Tyr (**5**) should also be better than that observed for the mixture of the four isomers used in this study.

Drug resistance is such a major problem for the control and treatment of malaria that novel targets and lead compounds for the development of new drugs are in continual demand.<sup>15</sup> This study establishes *PfLAP* as an antimalarial drug target by demonstrating a clear relationship between the ability of inhibitors to inactivate the enzyme and to kill malaria parasites in vitro and in vivo. It has been recently reported that methionine aminopeptidases are also promising targets for antimalarial development.<sup>16,17</sup> While studies in our laboratory have demonstrated little or no synergy between inhibitors of *PfLAP* and those of DV endopeptidases, falcipains and plasmepsins,<sup>18</sup> perhaps because these enzymes function in different cellular compartments, it is plausible that synergism would occur with *PfLAP* and methionine aminopeptidases inhibitors, raising the possibility of a combination drug therapy. It is also appropriate to mention that malaria parasites express three other aminopeptidases, a M1 alanyl aminopeptidase, a prolyl aminopeptidase, and an aspartyl aminopeptidase (plasmodb.org). Studies in our laboratory indicate that the M1 alanyl aminopeptidase is inhibited by the inhibitors described here; hence, its inactivation may be relevant to their antimalarial activity. The prolyl and aspartyl aminopeptidases, however, are not targets of these inhibitors and could also be exploited for future combination drug therapies.

Compounds **4** and **5** are the most potent inhibitors of M17 LAPs reported to date.<sup>6</sup> Their potency, together with their greater selectivity for *PfLAP* over bovine and porcine LAP, makes them attractive lead compounds for the development of antimalaria therapeutic agents. Although we observed no toxicity in the present in vivo studies, it is unknown if **4** and **5** will cause significant toxicity in humans. Bestatin has little toxicity in animals (LD<sub>50</sub> = >4000 mg/kg in mice<sup>19</sup>) and humans.<sup>20,21</sup> Clearly, more detailed information on the pharmacodynamic and pharmacokinetics properties of the inhibitors described in this study are required to understand their activity against malaria parasites and to guide future medicinal chemistry approaches to optimize their potency and properties.

## Experimental Section

**Synthesis of Compounds.** Compound **1** (bestatin, (–)-*N*-[(2*S*,3*R*)-3-amino-2-hydroxy-4-phenylbutyryl]-*L*-leucine) was obtained from Sigma-Aldrich, Sydney, Australia. Phoshinic pseudo-dipeptides **2–5** were synthesized in our laboratories according to the procedure described previously.<sup>6</sup> The only novel final compound (**2**) was obtained by standard deprotection of methyl 3-[[1-(*N*-benzyloxycarbonylamino)-4-phenylbutyl]hydroxyphosphiny]propionate (Cbz-hPheP[CH<sub>2</sub>]-Gly-OMe),<sup>22</sup> purified by means of the reverse phase HPLC, and separated as the trifluoroacetate after lyophilization. For the details of its synthesis and characterization, see the Supporting Information. The analogues **3–5** are fully characterized elsewhere.<sup>6</sup>

**Production and Isolation of Enzymatically Active Recombinant *PfLAP*.** The production of functionally active *PfLAP* in baculovirus-transformed insect cells along with its purification and biochemical characterization are described elsewhere.<sup>5</sup> Briefly, the pENTR construct housing *PfLAP* (Pf14\_0439, plasmodb.org), pENTR-LAP, was recombined with BaculoDirectC-Term linear DNA (Invitrogen Corp.) and transfected into Sf9 (*Spodoptera frugiperda*) cells. For protein expression, Sf9 insect cells were infected at the cell density of 3 × 10<sup>6</sup> cells/mL with *PfLAP* recombinant baculovirus at a moiety of infection of 2–5 PFU/cell. The infections were allowed to proceed for 48 h at 28 °C before the cell pellets were harvested by centrifugation at 8000g for 15 min at 4 °C and stored at –80 °C. The cell pellets were lysed into PBS, pH 7.3, by three cycles of freeze–thaw and sonication and then centrifuged at 15 000 rpm for 30 min at 4 °C. The supernatant was filtered through a 0.45 μm HA Millipore membrane, diluted

5-fold with 50 mM sodium phosphate buffer, pH 8.0, containing 300 mM sodium chloride and 10 mM imidazole, and passed over a nickel–agarose column (Qiagen) equilibrated with the same buffer. The column was then washed with 50 mM sodium phosphate buffer, pH 8.0, containing 300 mM sodium chloride and 20 mM imidazole and *PfLAP* eluted into 50 mM sodium phosphate buffer, pH 8.0, containing 300 mM sodium chloride and 250 mM imidazole. The eluate was dialyzed against PBS, pH 7.3, for 16 h.

**Enzymatic Assay, Substrate and Inhibitor Kinetics with Fluorogenic Peptide Substrates.** Rates of hydrolysis of the fluorogenic substrate H-Leu-7-amino-4-methylcoumarin (H-Leu-NHMec) were measured by monitoring the release of the –NHMec fluorogenic leaving group at an excitation wavelength of 370 nm and an emission wavelength of 460 nm using a Bio-Tek KC4 microfluorimeter. Recombinant *PfLAP* was activated in 50 mM Tris-HCl, pH 8.0, containing 1 mM CoCl<sub>2</sub> for 20 min prior to the addition of substrate (10 μM). Inhibitors were initially screened by adding these at various concentrations ranging from 10 to 001 μM to the assay mix 10 min prior to adding substrate.

The binding constant, *K<sub>i</sub>*, for the inhibition of *rPfLAP* by compounds **2–5** was determined at 37 °C in 50 mM Tris-HCl, pH 8.0, by measuring the initial rate *v<sub>i</sub>* over a range of inhibitor concentrations (2.44–78.13 nM). The enzyme concentration was 26 nM and the substrate concentration was varied (2.5–100 μM). *K<sub>i</sub>* was calculated from a plot of 1/*v<sub>i</sub>* versus inhibitor concentration [I] by the method of Dixon.<sup>23</sup> Because bestatin was found to be a time-dependent inhibitor of *rPfLAP*, the overall inhibition constant *K<sub>i</sub>*\* was determined by monitoring progress curves until a final steady-state velocity *v<sub>s</sub>* was reached. Progress curves were monitored at 2 μM substrate over a range of inhibitor concentrations (19.53–312.5 nM) and at a fixed enzyme concentration of 26 nM. The *K<sub>i</sub>*\* was calculated from a Dixon plot of 1/*v<sub>s</sub>* versus [I]. The dissociation constant *K<sub>i</sub>* was calculated from a Dixon plot of 1/*v<sub>i</sub>* versus [I] where *v<sub>i</sub>* is the rate from the initial portion of the progress curve.

To determine the mechanism by which bestatin binds enzyme, progress curves were fitted to the integrated rate equation

$$P = v_s t + (v_0 - v_s)(1 - e^{-k_{\text{obs}} t})/k_{\text{obs}}$$

where *P* is the amount of product formed at time *t*, *v<sub>0</sub>* and *v<sub>s</sub>* are the initial and final steady-state velocities, and *k<sub>obs</sub>* is the observed first-order rate constant for the establishment of the equilibrium between the initial (EI) and final (EI\*) enzyme–inhibitor complexes.<sup>24</sup> *k<sub>obs</sub>* values were plotted against [I], and the data were fitted to the equation

$$k_{\text{obs}} = k_6 \left[ \frac{1 + \frac{I}{K_i^*(1 + A/K_a)}}{1 + \frac{I}{K_i(1 + A/K_a)}} \right]$$

where *K<sub>a</sub>* is the Michaelis constant for substrate A, *K<sub>i</sub>* is the dissociation constant for the EI complex, and *K<sub>i</sub>*\* is the overall inhibition constant for the formation of EI\*. This equation describes *k<sub>obs</sub>* when formation of EI\* from the initial EI complex is slow, as outlined in Scheme 1.<sup>7</sup>

**Homology Modeling of *PfLAP* Structure and Calculation of Ligand Binding Mode.** Bovine lens aminopeptidase (BILAP, sequence and 3D structure coordinates subtracted from PDB file 1lcp) and *PfLAP* exhibited good sequence similarity: 38% overall sequence identity and 56% sequence similarity in the catalytic domain. The pairwise sequence alignment of *PfLAP* with BILAP was performed using ClustalW (<http://www.ebi.ac.uk/clustalw>) and was then applied to calculate the 3D model of the catalytic domain of *PfLAP* (residues 280–606) by employing the Modeller program<sup>25</sup> (<http://guitar.rockerfeller.edu/modeller.html>) with the default parameters.

The hydrogen atoms were added to the *PfLAP* model in the InsightII/Builder program (Molecular Simulations Inc, San Diego),

using the standard protonation states for amino acids at pH 7.0. The X-ray structure of the BILAP–LeuP complex (encoded as 1lcp in PDB) and the model of BILAP–LeuP[NH]Leu reported by our laboratory<sup>6</sup> allowed docking of **4** ((*R*)-hPheP[CH<sub>2</sub>]-(*R*)-Phe) to the *Pf*LAP binding site by superimposition of the BILAP–ligand complexes onto the *Pf*LAP model. The Leu side chains at the P1 at P1' positions of BILAP ligand LeuP[NH]Leu were replaced with hPheP and Phe side chain, respectively, to obtain the *Pf*LAP–**4** complex. Subsequently, the protein was soaked in a 5 Å layer of water molecules, and the complex was optimized using the Amber force field within the Discover/InsightII program (Molecular Simulations Inc., San Diego, CA). The backbone of the protein was kept frozen during the optimization process, while the protein side chains, inhibitor molecules, and water molecules were allowed to move. The distance constraints between the active site metal ions and their ligands, both protein amino acids and ligand atoms interacting with them, were applied with the force constants of 500 kcal/mol Å<sup>2</sup> during the energy minimization procedure. The switched smoothing function, with gradually reduced nonbonding interactions to zero from 18 Å inner radius to 20 Å outer radius, was applied during the simulations. The optimization was performed using the conjugate gradient algorithm until the maximum derivative was <0.02 kcal/mol Å.

Since the complex of BILAP–bestatin is not available, the X-ray structure of BILAP–amastatin (encoded as 1bl1 in PDB) was used to dock bestatin to the *Pf*LAP binding site. As a first step the BILAP–amastatin complex was superimposed onto the *Pf*LAP model, and then the Leu side chains at P1 and the Val side chain at P1' of amastatin were replaced with Phe and Leu, respectively, while P2' and P3' fragments were deleted. The optimization of bestatin in the *Pf*LAP binding site was performed in the same way as described above for **4**.

De novo flexible docking of **4** {(*R*)-hPheP[CH<sub>2</sub>]-(*R*)-Phe} and bestatin to *Pf*LAP was also carried out using the Glide program with the XP (extra precision) docking module.<sup>26</sup> The 100 lowest energy conformers (docking poses) of **4** and bestatin were saved and clustered using rms = 1.5 Å as a clustering criteria. The results of docking with Glide are described in the Supporting Information.

**In Vitro Sensitivity of *P. falciparum* to Inhibitors.** *P. falciparum* clones 3D7, D10, and Dd2 were derived from *P. falciparum* isolates NF58, FC27, and W2MEF, respectively, and were obtained from The Walter and Eliza Hall Institute, Melbourne, Australia. Parasites were cultured as described.<sup>27</sup> Stock solutions of inhibitors were prepared in 100% DMSO. Dilutions of all drugs were prepared from stock solutions in culture medium when required. Vehicle controls were included on each assay plate.

The in vitro sensitivity of each parasite population to the aminopeptidase inhibitor bestatin and the phosphinate analogues was determined using [<sup>3</sup>H]hypoxanthine incorporation.<sup>28</sup> Briefly, serial dilutions of each inhibitor were prepared in culture media (0.05–50 μM) and added with [<sup>3</sup>H]hypoxanthine (0.5 μCi/well) to asynchronous cultures at a 0.5% parasitemia and 2% hematocrit. After a 48 h incubation, the amount of [<sup>3</sup>H]hypoxanthine incorporation was measured, and the concentrations of inhibitor required to prevent incorporation by 50% (IC<sub>50</sub>) were determined by linear interpolation of inhibition curves.<sup>29</sup> Each assay was performed in triplicate on three separate occasions.

**In Vivo Studies against *P. c. chabaudi*.** The in vivo antimalarial activity of **1** and **4** was determined using the nonlethal *P. chabaudi* murine malaria model in 8-week-old C57BL/6J female mice. Compound **5** was not included in these trials due to issues of supply. Mice were housed in a reverse light cycle cabinet (daylight 10 p.m. to 10 a.m.) to ensure drug exposure during the trophozoite stages. Mice (average weight, ~20 g) were infected intravenously in the tail vein with 5 × 10<sup>5</sup> parasitized erythrocytes from an infected donor mouse. Drugs were diluted from stocks into PBS, pH 7.3, and treatment initiated 24 h postinfection. Groups of six mice received 2 mg of compound **4** or **1**, via interperitoneal injection, twice daily for 7 consecutive days. Control groups received PBS alone twice a day for 7 days or 0.1 mg of chloroquine in PBS once daily for 4 consecutive days. The parasitemia was

monitored from day 3 postinfection by daily microscopic examination of Giemsa-stained thin blood smears. Animals were housed in the Queensland Institute of Medical Research (QIMR) animal facility under specific-pathogen-free conditions. Ethical approval for all animal work was obtained from the QIMR Animal Ethics Committee using protocols complying with guidelines set out by the National Health and Medical Research Council of Australia Animal Code of Practice. Each experiment was performed on two separate occasions with similar results. As the peak parasitemia in control mice varied slightly in each experiment, data from only one experiment are shown.

**Acknowledgment.** J.P.D. and C.M.S. were supported by a Basic Research Grant obtained from Enterprise Ireland. J.P.D. is a recipient of the NSW Government BioFirst Award in Biotechnology (2004). K.R.T. and D.L.G. were supported by NHMRC program Grant 290208 and by a generous donation from Mark Nicholson, Alice Hill, and the Tudor Foundation. T.S.S.-A. is a recipient of a University of Queensland Postdoctoral Fellowship and a Ramaciotti Development Grant. J.L. and consumables for this work were funded by an Australian Research Council Discovery Project Grant DP0666128.

**Supporting Information Available:** The synthetic procedure and characterization of compound **2** and the results of docking experiments (LeuP to bLAP, **4** to *Pf*LAP, and bestatin to *Pf*LAP). This material is available free of charge via the Internet at <http://pubs.acs.org>.

## References

- Breman, J. G. The ears of the hippopotamus: Manifestations, determinants, and estimates of the malaria burden. *Am. J. Trop. Med. Hyg.* **2001**, *64* (1–2 Suppl), 1–11.
- Yamey, G. Roll Back Malaria: A failing global health campaign. *BMJ [Br. Med. J.]* **2004**, *328* (7448), 1086–7.
- Gardiner, D. L.; Trenholme, K. R.; Skinner-Adams, T. S.; Stack, C. M.; Dalton, J. P.; Overexpression, of leucyl aminopeptidase in *Plasmodium falciparum* parasites. Target for the antimalarial activity of bestatin. *J. Biol. Chem.* **2006**, *281* (3), 1741–5.
- Rosenthal, P. J. Hydrolysis of erythrocyte proteins by proteases of malaria parasites. *Curr. Opin. Hematol.* **2002**, *9* (2), 140–5.
- Stack, C. M.; Lowther, J.; Cunningham, E.; Donnelly, S.; Gardiner, D. L.; Trenholme, K. R.; Skinner-Adams, T. S.; Teuscher, F.; Grembecka, J.; Mucha, A.; Kafarski, P.; Lua, L.; Bell, A.; Dalton, J. P.; Characterization, of the *Plasmodium falciparum* M17 leucyl aminopeptidase. A protease involved in amino acid regulation with potential for antimalarial drug development. *J. Biol. Chem.* **2007**, *282* (3), 2069–80.
- Grembecka, J.; Mucha, A.; Cierpicki, T.; Kafarski, P. The most potent organophosphorus inhibitors of leucine aminopeptidase. Structure-based design, chemistry, and activity. *J. Med. Chem.* **2003**, *46* (13), 2641–55.
- Duggleby, R. G.; Attwood, P. V.; Wallace, J. C.; Keech, D. B. Avidin is a slow-binding inhibitor of pyruvate carboxylase. *Biochemistry* **1982**, *21* (14), 3364–70.
- Burley, S. K.; David, P. R.; Sweet, R. M.; Taylor, A.; Lipscomb, W. N. Structure determination and refinement of bovine lens leucine aminopeptidase and its complex with bestatin. *J. Mol. Biol.* **1992**, *224* (1), 113–40.
- Kim, H.; Lipscomb, W. N. X-ray crystallographic determination of the structure of bovine lens leucine aminopeptidase complexed with amastatin: Formulation of a catalytic mechanism featuring a gem-diolate transition state. *Biochemistry* **1993**, *32* (33), 8465–78.
- Strater, N.; Lipscomb, W. N. Transition state analogue L-leucine-phosphonic acid bound to bovine lens leucine aminopeptidase: X-ray structure at 1.65 Å resolution in a new crystal form. *Biochemistry* **1995**, *34* (28), 9200–10.
- Liu, J.; Istvan, E. S.; Gluzman, I. Y.; Gross, J.; Goldberg, D. E. *Plasmodium falciparum* ensures its amino acid supply with multiple acquisition pathways and redundant proteolytic enzyme systems. *Proc. Natl. Acad. Sci. U.S.A.* **2006**, *103* (23), 8840–5.
- Gavigan, C. S.; Dalton, J. P.; Bell, A. The role of aminopeptidases in haemoglobin degradation in *Plasmodium falciparum*-infected erythrocytes. *Mol. Biochem. Parasitol.* **2001**, *117* (1), 37–48.
- Scornik, O. A.; Botbol, V. Cellular uptake of 3H-bestatin in tissues of mice after its intravenous injection. *Drug Metab. Dispos.* **1997**, *25* (7), 798–804.

- (14) Suda, H.; Aoyagi, T.; Takeuchi, T.; Umezawa, H. Inhibition of aminopeptidase B and leucine aminopeptidase by bestatin and its stereoisomer. *Arch. Biochem. Biophys.* **1976**, *177* (1), 196–200.
- (15) Nwaka, S.; Hudson, A. Innovative lead discovery strategies for tropical diseases. *Nat. Rev. Drug Discovery* **2006**, *5* (11), 941–55.
- (16) Chen, X.; Chong, C. R.; Shi, L.; Yoshimoto, T.; Sullivan, D. J.; Jr.; Liu, J. O. Inhibitors of *Plasmodium falciparum* methionine aminopeptidase 1b possess antimalarial activity. *Proc. Natl. Acad. Sci. U.S.A.* **2006**, *103* (39), 14548–53.
- (17) Gavigan, C. S.; Machado, S. G.; Dalton, J. P.; Bell, A. Analysis of antimalarial synergy between bestatin and endoprotease inhibitors using statistical response-surface modelling. *Antimicrob. Agents Chemother.* **2001**, *45* (11), 3175–81.
- (18) Skinner-Adams, T. S.; Andrews, K. T.; Melville, L.; McCarthy, J.; Gardiner, D. L. Synergistic interactions of the antiretroviral protease inhibitors saquinavir and ritonavir with chloroquine and mefloquine against *Plasmodium falciparum* in vitro. *Antimicrob. Agents Chemother.* **2007**, *51* (2), 759–62.
- (19) Sakakibara, T.; Ito, K.; Irie, Y.; Hagiwara, T.; Sakai, Y.; Hayashi, M.; Kishi, H.; Sakamoto, M.; Suzuki, M.; Irie, Y.; et al. Toxicological studies on bestatin. I. Acute toxicity test in mice, rats and dogs. *Jpn. J. Antibiot.* **1983**, *36* (11), 2971–84.
- (20) Scornik, O. A.; Botbol, V. Bestatin as an experimental tool in mammals. *Curr. Drug Metab.* **2001**, *2* (1), 67–85.
- (21) Ichinose, Y.; Genka, K.; Koike, T.; Kato, H.; Watanabe, Y.; Mori, T.; Iioka, S.; Sakuma, A.; Ohta, M., Randomized double-blind placebo-controlled trial of bestatin in patients with resected stage I squamous-cell lung carcinoma. *J. Natl. Cancer Inst.* **2003**, *95* (8), 605–10.
- (22) Mucha, A.; Pawel, M.; Hurek, J.; Kafarski, P. Synthesis and activity of phosphinic tripeptide inhibitors of cathepsin C. *Bioorg. Med. Chem. Lett.* **2004**, *14* (12), 3113–6.
- (23) Dixon, M. The determination of enzyme inhibitor constants. *Biochem. J.* **1953**, *55* (1), 170–1.
- (24) Morrison, J. F.; Walsh, C. T. The behavior and significance of slow-binding enzyme inhibitors. *Adv. Enzymol. Relat. Areas Mol. Biol.* **1988**, *61*, 201–301.
- (25) Sali, A.; Blundell, T. L. Comparative protein modelling by satisfaction of spatial restraints. *J. Mol. Biol.* **1993**, *234* (3), 779–815.
- (26) Friesner, R. A.; Murphy, R. B.; Repasky, M. P.; Frye, L. L.; Greenwood, J. R.; Halgren, T. A.; Sanschagrin, P. C.; Mainz, D. T. Extra precision glide: Docking and scoring incorporating a model of hydrophobic enclosure for protein-ligand complexes. *J. Med. Chem.* **2006**, *49* (21), 6177–96.
- (27) Trager, W.; Jensen, J. B. Human malaria parasites in continuous culture. *Science* **1976**, *193* (4254), 673–5.
- (28) Geary, T. G.; Divo, A. A.; Jensen, J. B. An in vitro assay system for the identification of potential antimalarial drugs. *J. Parasitol.* **1983**, *69* (3), 577–83.
- (29) Huber, W.; Koella, J. C. A comparison of three methods of estimating EC50 in studies of drug resistance of malaria parasites. *Acta Trop.* **1993**, *55* (4), 257–61.

JM070733V